Search for direct stau pair production in final states with at least one hadronically decaying tau at $\sqrt{s}$ =13TeV and 80 fb^{-1} in ATLAS

Supervisor: Dr. Stefan Guindon, Dr. Javier Montejo

CERN summer student: Jiashen Tang

Abstract

A search for direct stau pair production with Monte Carlo proton-proton collisions at a center-of-mass energy of 13 TeV and luminosity of 80 fb^{-1} is presented. This process is characterized by final states with at least one hadronically decaying tau lepton and missing transverse momentum. Stransverse mass M_{T2} and summation of transverse mass $\sum M_T$ are exploited as discriminating variables. In two hadronically decaying tau channel, a search region with M_{T2} > 90GeV and $|\Delta\varphi(\tau_1, \tau_2)|$ > 1.5 using di-tau+ E_T^{miss} trigger is found to have $s/\sqrt{B} \approx 4$, indicating a potential supersymmetry tau discovery region.

1 Introduction

Supersymmetry (SUSY), based on the symmetry between fermions and bosons [1], is a promising extension to Standard Model (SM). It postulates the existence of a partner state for every SM particle with same quantum number, except for spin which differs by one half unit. Certain classes of SUSY models can lead to unification of gauge coupling at high energy [2], provide a solution to hierarchy problem without fine tuning by stabilizing the mass of the Higgs boson against large radiative corrections [3]. In R-parity conserving models, supersymmetric particles are always produced in pairs, the lightest supersymmetry particle (LSP) is stable and considered to be the candidate of dark matter [3].

In various SUSY scenarios, the lightest SUSY particles of SM lepton families are those of third-generation, resulting in a stau (labeled as $\tilde{\tau}$) rich final states [4]. It plays a role in co-annihilation with neutrolino leading to a dark matter density relic consistent with current cosmological observation [4].

Previously search for SUSY particles including charginos ($\tilde{\chi}_i^{\pm}, i = 1,2$), neutrolinos ($\tilde{\chi}_j^0, j = 1,2,3,4$) and sleptons ($\tilde{l}, \tilde{\nu}$) are described in ref. [1-6]. Production of stau pairs has smaller cross section compared to $\tilde{\chi}_1^{\pm}\tilde{\chi}_1^{\mp}$ and $\tilde{\chi}_1^{\pm}\tilde{\chi}_2^0$ in *pp* collision. However, if mass of chargino and neutrolino are high and inaccessible at LHC. Then the dominant SUSY process should be stau pair production [7].

In this report, the search for direct stau pair production with Monte Carlo proton-proton collision, as shown in Figure 1 [1], at $\sqrt{s}$= 13TeV 80fb^{-1} will be presented. Stau ($\tilde{\tau}$) will decay to neutrolino ($\tilde{\chi}_1^0$,LSP) and SM tau (τ) with 100% branching ratio. The final state contains at least one hadronically decaying tau (τ_{h}) and missing transverse momentum (E_T^{miss}), i.e. either two taus decay hadronically ($\tau_{\mathrm{h}}\tau_{\mathrm{h}}$, channel) or one decays hadronically and the other decays leptonically ($l\tau_{\mathrm{h}}$ channel, *l* stands for electron or muon). This search will make use of stransverse mass (M_{T2}) and summation of transverse mass ($\sum M_{\mathrm{T}}$), which tries to estimate mass of two identical heavier mother particles when both decay to one visible and one invisible lighter particles. In this search, the visible particle is reconstructed τ lepton and the invisible one is neutrolino.

This report is organized as follows: A brief description of ATLAS detector and event reconstruction are presented in section 2 and 3. Monte Carlo event generation is listed in section 4. Trigger and event selection are discussed in section 5 and 6. Section 7 outlines background estimation relevant to direct stau search process. Section 8 is a summary of search results.

My project includes particle kinetic information study, trigger system efficiency comparison and selection, and finally I discovered a potential supersymmetry tau discovery region for two hadronically decaying tau channel.

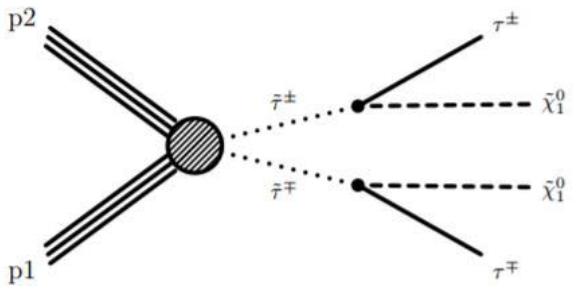

Figure 1: Schematic pair production of τ pairs from simplified model of direct stau production.

2 The ATLAS detector

The ATLAS detector [8] is a multipurpose particle physics detector. It covers a nearly 4π solid angle, features an inner tracking detector (ID), electromagnetic (EM) and hadronic (HAD) calorimeters, and a muon spectrometer (MS). ID, surrounded by a 2T superconducting solenoid, consists of a silicon pixel detector, a semiconductor microstrip detector and a transition radiation tracker. They cover a pseudorapidity region $|\eta| < 2.5$. The electromagnetic calorimeters (ECAL) are composed of high granularity liquid-argon (LAr) with lead, copper, or tungsten absorbers and measures the energy and position of shower within $|\eta| < 3.2$. Hadronic calorimeter is composed of steel/scintillator tile and measures the shower energy in the region $|\eta| < 1.7$ while a sampling calorimeter is deployed in the end-cap and forward regions spanning $1.5 < |\eta| < 4.9$. The MS surrounds the calorimeters and consists of three large superconducting air-core toroid magnets, each with eight coils, a system of precision tracking chambers ($|\eta| < 2.7$), and detectors for triggering ($|\eta| < 2.4$). Events are selected by a three-level trigger system.

3 Event reconstruction

3.1 Reconstruction of tau

With a mass of 1.777GeV and proper decay of 87μm, tau leptons decay either hadronically ($\tau \rightarrow$hadrons+ν_τ) or leptonically ($\tau \rightarrow l+\nu_l+\nu_\tau$, where l stands for electron or muon) before reaching active detecting materials [9]. Therefore, they can only be identified via decay products. For hadronically decay tau, most hadrons consist of charged and neutral pions. They make up the visible decay products of tau leptons and are labeled as $\tau_{\text{had-vis}}$.

Jets are hadron sprays and are first reconstructed using three-dimensional clusters of calorimeter cells and anti-k_t (see ref. [10]). Individual jets satisfying p_{T} and $|\eta|$ requirements will be used to as seeds for $\tau_{\text{had-vis}}$ reconstruction algorithm. All the tau candidate tracks with $p_{\text{T}} > 1$ GeV and satisfying additional requirements on number of hits in ID and angular separation ΔR around jet seed direction will be used as inputs for tau vertex (TV) association algorithm (details in ref. [11]). In events with multiple simultaneous pp collision (pile-up), the tau production vertex returned by TV association algorithm may not be the real vertex. To reduce pile-up effect, the primary vertex is chosen to be the one with highest $\sum p_{T,tracks}^2$,i.e. the transverse momentum sum of all tracks associated with TV. For physics analysis with high p_T events, such vertex coincides 99% with real production vertex. TV is used to build new coordinate system for re-calculating the four-momentum and direction of $\tau_{\text{had-vis}}$ candidates. Additional tracks (jets not associated with primary

vertex, leptons and photons etc.) are associated with $\tau_{\text{had-vis}}$ if their angular separation $\Delta R < 0.2$ (core region) with other criteria on p_{T}, number of hits in ID and impact parameter w.r.t. TV. Tracks in $0.2 < \Delta R < 0.4$ around $\tau_{\text{had-vis}}$ are used for calculation of identification variables which will be used in discrimination against jets from background events [9].

3.2 Discrimination against background jets, electrons and muons

Background jets Background jets are dominated by quarks and gluons' hadronization. Real $\tau_{\text{had-vis}}$ is more collimated and has less associated tracks, which can be exploited to discriminate against background jets. Discriminating variables including fraction of transverse energy deposited in $\Delta R < 0.1$ w.r.t. $\Delta R < 0.2$ ($\boldsymbol{f_{cent}}$), number of tracks in isolation area (N_{track}^{iso}) and the highest-p_{T} fraction w.r.t. the transverse energy sum in core region ($\boldsymbol{f_{track}}$) etc. are combined in Boosted Decision Tree (BDT) training to effectively reject $\tau_{\text{had-vis}}$ from background jets. Depending on the tightness of BDT identification criteria, three different working points, *tight*, *medium* and *loose*, are labeled corresponding to different tau identification efficiency [9].

Electron veto To prevent electron being mis-identified as 1-track $\tau_{\text{had-vis}}$ candidates, different algorithm and BDT are devoted to exploit the following variables: transition radiation, more likely to be emitted by electrons; large ΔR between $\tau_{\text{had-vis}}$ direction; more energy deposition in electromagnetic calorimeter compare to total energy deposited in EM+HAD calorimeter etc [9].

Muon veto Muon are unlikely to be reconstructed as $\tau_{\text{had-vis}}$, as they barely deposit enough energy in calorimeter. For sufficiently energetic muon, they register a less fraction of energy in EM calorimeter and have a high track-p_T to E_{T} ratio. Low energy muons that are stopped at HAD calorimeter are characterized by higher energy fraction in EM calorimeter and a low ratio of track-p_T to E_{T}. Simple cut method could already reduce muon contamination to negligible level [9].

3.3 Reconstruction of electron and muon

Electron and muon are identified using specific detector signatures. Electrons are reconstructed by matching track from ID and an energy deposition in ECAL. Muon are reconstructed by matching track from ID and its extrapolation to MS [1-5,9].

4 Monte Carlo simulation

Monte Carlo generator are used to simulate target SUSY events and background SM processes. Only SM processes have similar signatures with final states as SUSY signals are considered. W+jets and Z+jets are simulated from Sherpa 2.2.1. $t\bar{t}$ events are obtained from Powheg ($\tau_{\text{h}}\tau_{\text{h}}$ channel) and Pythia8($l\tau_{\text{h}}$ channel). SUSY events, stau mass 120GeV and 180GeV, are generated by Madgraph and Pythia8.

5 Trigger selection

In LHC data taking period, only interested events satisfying trigger requirements based on their kinematics are stored to handle bandwidth limits, time constraints and incomplete reconstruction of tau at trigger level [9]. In my study, the kinematic behavior of decay products of $\tilde{\tau}$ (180GeV) and $\tilde{\tau}$ (120GeV) with $\tilde{\chi}_1^0$(1GeV) differs slightly and the same trigger is applied to both. All possible

lowest unprescaled triggers are tested for $\tilde{\tau}$ (180GeV) signal acceptance comparison are tabulated in Table 1.

Table 1: Tau triggers with their corresponding kinematic requirements for $\tilde{\tau}$ (180GeV) $\tilde{\chi}_1^0$(1GeV)

$\tau_h\tau_h$ Channel	
Trigger	**Signal acceptance**
$p_T(\tau_1)$>120GeV $p_T(\tau_2)$>80GeV	7%
$p_T(\tau_1)$>55GeV $p_T(\tau_2)$>40GeV ΔR<2.6	10%
$p_T(\tau_1)$>55GeV E_T^{miss}>100GeV	19%
$p_T(\tau_1)$>55GeV $p_T(\tau_2)$>40GeV E_T^{miss}>75GeV	20%
$p_T(\tau_1)$>55GeV E_T^{miss}>150GeV	6%
$p_T(\tau_1)$>55GeV $p_T(\tau_2)$>40GeV E_T^{miss}>125GeV	6%
$l\tau_h$ Channel	
Trigger	**Signal acceptance**
$p_T(l)$>27GeV	73%
$p_T(\tau)$>120GeV $p_T(e)$>19GeV	6%
$p_T(\tau)$>55GeV $p_T(\mu)$>15GeV	28%
$p_T(\tau)$>40GeV $p_T(e)$>19GeV E_T^{miss}>80GeV	11%
$p_T(\tau)$>40GeV $p_T(\mu)$>15GeV E_T^{miss}>80GeV	14%
$p_T(\tau)$>40GeV $p_T(e)$>19GeV E_T^{miss}>130GeV	5%
$p_T(\tau)$>40GeV $p_T(\mu)$>15GeV E_T^{miss}>130GeV	4%

For final states with two hadronically decaying tau ($\tau_h\tau_h$ Channel), the best signal acceptance is $p_T(\tau_1)$ > 55GeV, $p_T(\tau_2)$ > 40GeV and E_T^{miss}> 75GeV. However, $E_T^{miss}$is not fully efficient before ~130GeV where it reaches a plateau. Therefore, to efficient use trigger selection, E_T^{miss}needs to be promoted to ~150GeV, which lead to a huge plummet in signal acceptance. To compensate the lost data, the trigger lessened requirement for di-tau is used and the final trigger in this analysis is $p_T(\tau_1)$ > 40GeV, $p_T(\tau_2)$ > 30GeV and E_T^{miss}> 130GeV.

For final states with one hadronically decay and one leptonically decay tau ($l\tau_h$ Channel), single lepton trigger already demonstrate an excellent performance. To suppress additional backgrounds, we will also require information on a high $p_T(\tau)$ and E_T^{miss}. The final trigger is $p_T(\tau)$ > 20GeV, $p_T(l)$ > 27GeV and E_T^{miss}> 50GeV in search region 1 (defined in section 6) and $p_T(\tau)$ > 70GeV, $p_T(l)$ > 50GeV and E_T^{miss}> 100GeV in search region 2 (tighter constraint, defined in section 6)

6 Event selection

After passing trigger requirements, events are further selected to reduce relevant background. Discriminating variables includes work point of BDT *tight, medium, loose*, charge sign of tau pairs, b-tagged jets (using combined secondary vertex (CSV) algorithm by exploiting life-time information) veto, and impact parameter w.r.t TV, angular separation $\Delta\varphi$ $\Delta\eta$ between $\tau_h\tau_h$ or $l\tau_h$ as Drell-Yan process have back-to-back tau pairs [3, 9]. To further background events, we will make use of stransverse mass M_{T2} [12] which is an extension of transverse mass M_T.

For a mother particle decays to a visible and an invisible particle, $\tilde{\tau} \to \tau + \tilde{\chi}_1^0$ in our case. Transverse mass M_T is defined as:

$$M_T\left(\vec{p}_T^{\,\tau}, \vec{p}_T^{\,\tilde{\chi}_1^0}; m_{\tilde{\chi}_1^0}\right) = \sqrt{m_\tau^2 + m_{\tilde{\chi}_1^0}^2 + 2\left(E_T^\tau E_T^{\tilde{\chi}_1^0} - \vec{p}_T^{\,\tau}\vec{p}_T^{\,\tilde{\chi}_1^0}\right)} \quad (1)$$

$$E_T^{\tilde{\chi}_1^0} = \sqrt{(\vec{p}_T^{\,\tilde{\chi}_1^0})^2 + m_{\tilde{\chi}_1^0}^2} \quad (2)$$

m_τ=1.777GeV and $m_{\tilde{\chi}_1^0}$=1GeV, which are negligible compared to stau mass. The magnitude of $\vec{p}_T^{\,\tilde{\chi}_1^0}$ is E_T^{miss}. Both hadronic and leptonic decay mode of tau contains neutrino, which carries additional momentum that will be absorbed in E_T^{miss}. Besides, the momentum of tau is partially reconstructed due to our lack of knowledge of neutrino kinematics. But nevertheless, the distribution of M_T has a kinematic end point at the mass of mother. In this analysis, mother particles are two tau sleptons produced in pairs and both decay to visible tau and invisible neutrolino. E_T^{miss} is the magnitude of vector sum of two invisible neutrolinos plus extra neutrinos. The variable $\sum M_T$, a combination of $M_T(\tau_1, \vec{p}_T^{\text{miss}})$ and $M_T(\tau_2, \vec{p}_T^{\text{miss}})$, is used and the distribution is shown in Figure 2(Left). A requirement on high $\sum M_T$ significantly reduces SM background.

As E_T^{miss} is the momentum summation of all invisible particles. One cannot use $\sum M_T$ to estimate mass of mother particle, stau. In such case, M_{T2} tries to get a handle on the mass of initial pair-produced particles. It is defined as:

$$M_{T2} = \min_{\vec{p}_T^{\,x(1)} + \vec{p}_T^{\,x(2)} = \vec{p}_T^{\,\text{miss}}} \left[\max(M_T^{(1)}, M_T^{(2)})\right] \quad (3)$$

Where $\vec{p}_T^{\,x(i)}$ (i=1,2) is the transverse momentum of two undetected neutrolinos which parametrize our lack of knowledge about true neutrolino momenta. $M_T^{(1)}$ and $M_T^{(2)}$ are calculated by pairing with all possible combinations of $\vec{p}_T^{\,x(i)}$ which should sum up to E_T^{miss}. The distribution of M_{T2} is presented in Figure 2(Right). A high requirement will greatly reduce background events but also reduce the signal acceptance for lower stau mass case.

One can clearly observe a high rate when $\sum M_T \to 0$ and $M_{T2} \to 0$. This is the case when two taus are produced back-to-back with almost identical momenta, where no E_T^{miss} will be reconstructed since it is computed as a negative vector sum of all visible tracks associated with tau vertex. This situation coincides with Drell-Yan process [9].

$\tau_h\tau_h$ Channel

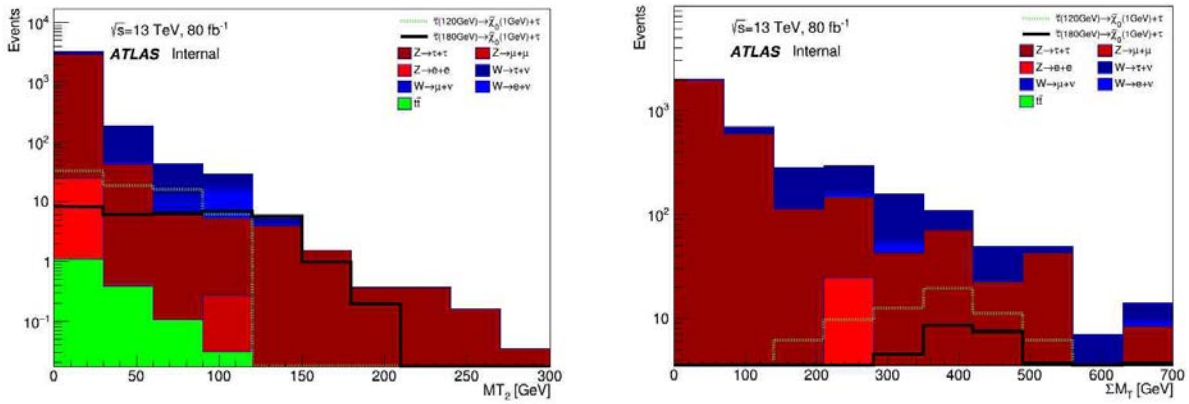

$l\tau_h$ Channel

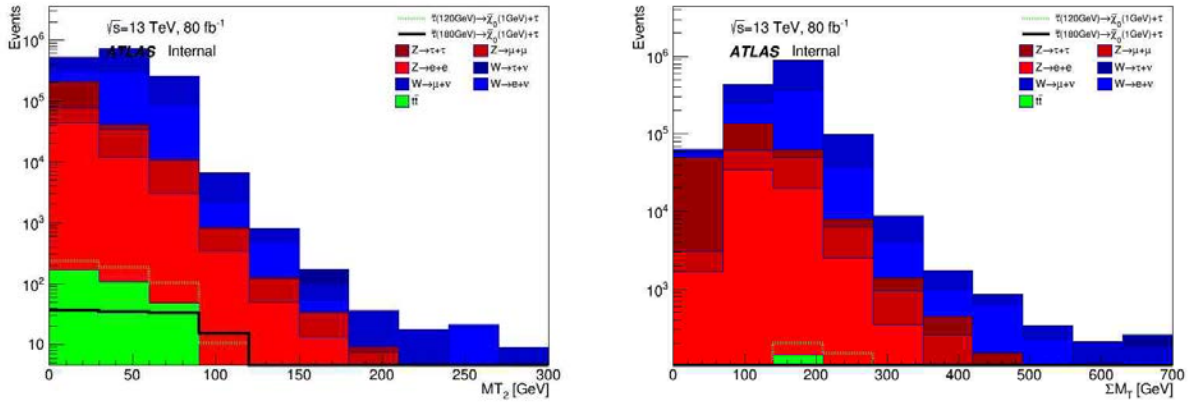

Figure 2: $M_{T2}$and $\sum M_T$ distribution. Upper panel is $\tau_h\tau_h$ channel lower panel is $l\tau_h$ channel

Different search regions are defined to target at heavy and light stau mass for both $\tau_h\tau_h$ and $l\tau_h$ Channel, as high requirement on $\sum M_T$, M_{T2}will have different discrimination performance for various stau mass. The search region used in this analysis are:

$\tau_h\tau_h$ Channel		
Search region 1	**Search Region 2**	**Search Region 3**
$\sum M_T$ > 90GeV	40GeV < M_{T2} < 90GeV	40GeV < M_{T2} < 90GeV
$\lvert\Delta\varphi(\tau_1, \tau_2)\rvert$ > 1.5	$\sum M_T$> 350GeV	300GeV < $\sum M_T$< 350GeV
	E_T^{miss}> 50GeV	E_T^{miss}> 50GeV
	$\lvert\Delta\varphi(\tau_1, \tau_2)\rvert$ > 1.5	$\lvert\Delta\varphi(\tau_1, \tau_2)\rvert$ > 1.5

$l\tau_h$ Channel	
Search region 1	**Search Region 2**
M_{T2} > 70GeV	M_{T2} > 90GeV
$\sum M_T$> 200GeV	$\sum M_T$> 400GeV
$\lvert\Delta\varphi(\tau, l)\rvert$ > 1.5	$\lvert\Delta\varphi(\tau, l)\rvert$ > 1.5

7 Background estimation

Background from Monte Carlo simulation using production cross section may not coincide well with data, due to imperfection of modeling. Several methods have been developed to match LHC data with Monte Carlo simulation.

Background can be characterized as "misidentified" τ_h candidate, where quark or gluon jets are misidentified as τ_h, and "true" τ_h. After requiring a large transverse momentum $p_T(\tau)$, the dominant background consists of QCD multijet, W+jets (misidentified τ_h) and $t\bar{t}$, Z+jets and diboson events (true τ_h) [1-5].

QCD multijet has a large production cross section and contributes 13% to 30% [3] to total background. They are estimated from data using "ABCD" method due to poor MC model of misidentification. Three control region ABC is used to estimate multijet events in signal region D. The idea is (details in ref. [2-5]) to define such four regions in 2-dimensional plane using tau isolation criteria and kinematic variable e.g. M_{T2}. Four regions are exclusive and represent different level of QCD multijet activity. A D region has high requirement on kinematic variable compared to B C. From A to D and B to C, reconstructed taus are required to pass *tight* BDT requirements. The fraction of events passing *tight* requirements in B or A are found to be independent of kinetmatic variable. Therefore, number of misidentified tau, i.e. multijet events, in D can be estimated by a transfer factor $N_D = N_A \times N_C/N_B$.

W+jets contributes 25% to 50% to background events [3]. It is estimated by defining a specific control region which will be used to normalize MC simulation to data (details in ref. [2-5]). The control region requires minimal contamination from other backgrounds. Events with exactly one isolated muon and one tau passing tight jet BDT requirements are selected to suppress QCD multijet events. Invariant mass of two leptons are required to be outside Z mass window to reduce Z jets contamination. Events with *b*-tagged jets are veto to constrain top quarks interaction. Additional requirements on angular separation and E_T^{miss} are applied to further suppress other background contamination.

Irreducible true τ_h background including diboson ($WW \rightarrow \tau\nu\tau\nu$ and $ZZ \rightarrow \tau\nu\tau\nu$), $t\bar{t}$ and Drell-Yan ($Z/\gamma \rightarrow \tau\tau \rightarrow \tau_h\tau_h$ and $Z/\gamma \rightarrow \tau\tau \rightarrow l\tau_h$) are estimated from MC simulation and validated in data (details in ref. [2-5]).

8 Results Summary

The distributions of background and SUSY events after selection applied in each search region are presented in Figure 3 below.

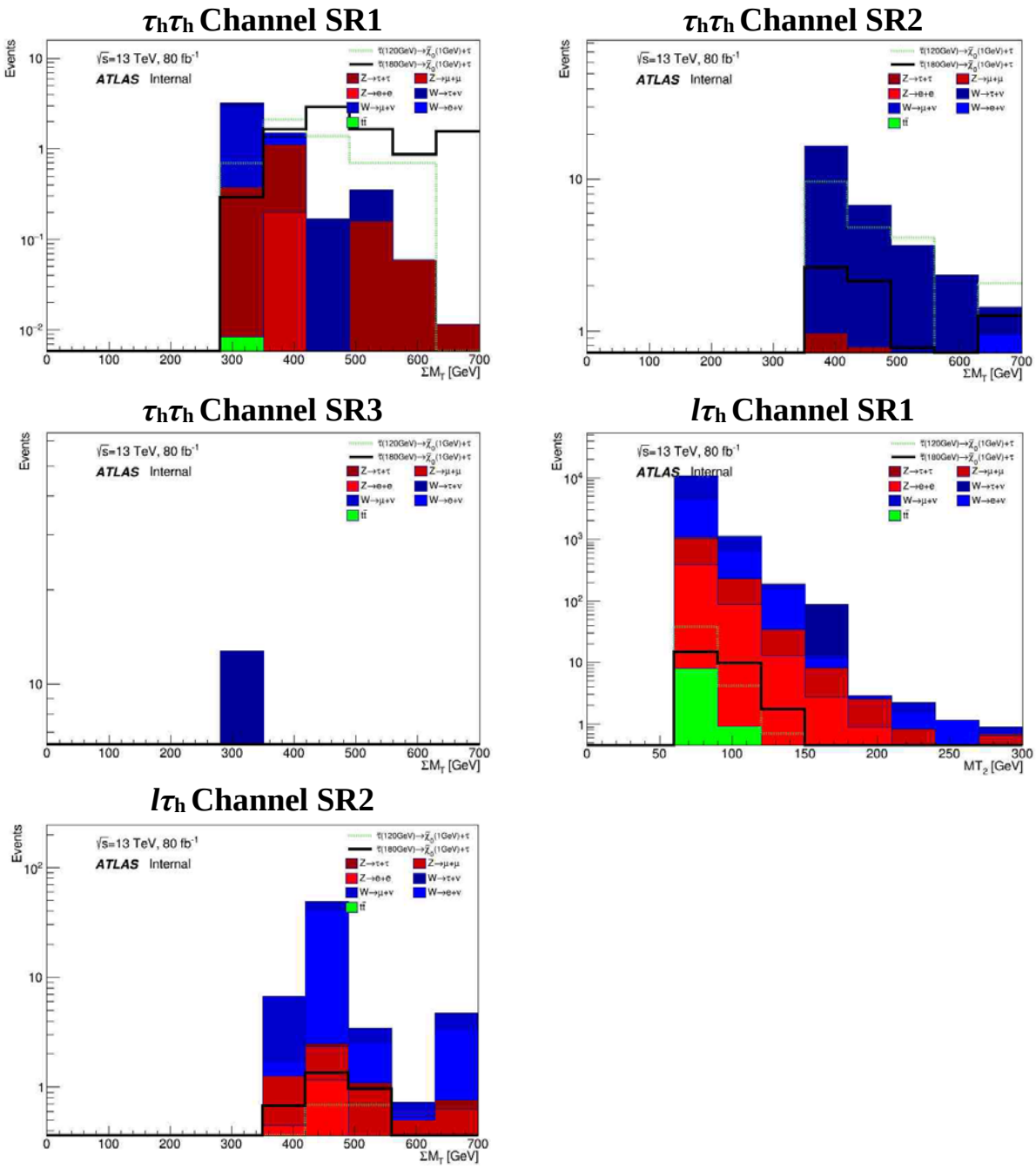

Figure 3:M_{T2} distribution for signal versus background. $l\tau_h$ has much more background than $\tau_h\tau_h$

In $\tau_h\tau_h$ search region 1, tight require on M_{T2} gives a better signal sensitivity for higher stau mass. $s/\sqrt{B} \approx 4$ suggests a potential supersymmetry tau discovery region, however, a tight constraint lead to fewer MC data for further optimization and background fluctuation may dissembled

discovery of signal events. Fake tau rate should be checked from data as MC modeling is insufficient. QCD multijet background needs also to be incorporated to check performance of current search region

In $l\tau_h$ channel, signal is submerged in large background events even for much tighter search region 2 (W+jets is dominant). A detailed investigation on current and new discrimination variables exploiting the topology of W+jets, Z+jets events and recalculation of $E_{\mathrm{T}}^{\mathrm{miss}}$to improve the long tail of M_{T2} distribution could be explored for further investigation.

9 Acknowledgement

Many thanks to Dr. Stefan Guindon, Dr. Javier Montejo and Pieter Everaerts from CERN and Prof. Luis Roberto Flores-Castillo, Prof. Ming-Chung Chu from CUHK for providing generous help and guide on this summer project. The funding and supports are also provided by CERN summer student project and CN Yang Scholarhship, CUHK.

References

[1] CMS Collaboration, "Search for pair production of tau sleptons in $\sqrt{s}$ = 13 TeV pp collisions in the all-hadronic final state", CMS Physics Analysis Summary CMS-PAS-SUS-17-003, 2017.

[2] CMS Collaboration, "Search for electroweak production of charginos in final states with two tau leptons in pp collisions at $\sqrt{s}$ = 8 TeV", JHEP 04 (2017) 018, doi:10.1007/JHEP04(2017)018, arXiv:1610.04870.

[3] ATLAS Collaboration, "Search for the direct production of charginos, neutralinos and staus in final states with at least two hadronically decaying taus and missing transverse momentum in pp collisions at $\sqrt{s}$ = 8 TeV with the ATLAS detector", JHEP 10 (2014) 96, doi:10.1007/JHEP10(2014)096, arXiv:1407.0350.

[4] ATLAS Collaboration, "Search for the electroweak production of supersymmetric particles in $\sqrt{s}$ = 8 TeV pp collisions with the ATLAS detector", Phys. Rev. D 93 (2016) 052002, doi:10.1103/PhysRevD.93.052002, arXiv:1509.07152.

[5] ATLAS collaboration, Search for direct production of charginos and neutralinos in events with three leptons and missing transverse momentum in $\sqrt{s}$ = 8 TeV pp collisions with the ATLAS detector, JHEP 04 (2014) 169, arXiv:1402.7029.

[6] ATLAS collaboration, ATLAS Run 1 searches for direct pair production of third-generation squarks at the Large Hadron Collider, Eur. Phys. J. C 75 (2015) 510, arXiv:1506.08616.

[7] H. Baer, C.-h. Chen, F. Paige and X. Tata, Detecting sleptons at hadron colliders and supercolliders, Phys. Rev. D 49 (1994) 3283, arXiv:hep-ph/9311248

[8] ATLAS collaboration, The ATLAS experiment at the CERN Large Hadron Collider, Eur. Phys. J. C75 (2015) 303, arXiv:1207.7214.

[9] ATLAS collaboration, Identification and energy calibration of hadronically decaying tau leptons with the ATLAS experiment in pp collisions at $\sqrt{s}$ =8 TeV, 2008 JINST 3 S08003 arXiv:1207.7214

[10] M. Cacciari, G.P. Salam and G. Soyez, The anti-kt jet clustering algorithm, JHEP 04

(2008) 063, arXiv:0802.1189

[11] ATLAS Collaboration, ATLAS-CONF-2014-018 (2014), [http://cds.cern.ch/record/1700870]

[12] Alan Barr, Christopher Lester, Phil Stephens, m_{T2} : the truth behind the glamour J.Phys.G29:2343-2363,2003, arXiv:hep-ph/0304226